

# Robustness of an All-Optical Limiter to Manufacturing Errors

Frederique Gadot and Geraldine Guida\*

LEME, EA 4416, 50 Rue de Sèvres, Université Paris Nanterre — UPN, 92410, Ville d'Avray, France

**ABSTRACT:** In this paper, we present a numerical study to assess the robustness of an all-optical photonic limiter based on a two-dimensional (2D PC)  $\text{TiO}_2$  photonic crystal with a single ZnO nonlinear two-photon absorption (TPA) defect to manufacturing disturbances. These disturbances studied here concern diameters and positions. It is revealed that our limiter configuration is very robust to manufacturing errors.

## 1. INTRODUCTION

Photonic crystals (PCs) have been extensively studied over the past decades [1]. In most cases, PCs are considered to be perfect periodic arrays. Nevertheless, studies have revealed that their properties generally remain robust when manufacturing errors occur [2–4]. Several studies of perturbations in periodic structures have been performed in the microwave and far-infrared range where manufacturing errors can be managed or occur [5, 6]. However, to our knowledge, the study of perturbations of different parameters on an all-optical limiter has not yet been carried out.

One of the first 2D PC limiters in the visible range was proposed by Lin et al. [7] using a thermal nonlinear liquid. All-optical limiters consisting of 1D PC with solid materials have been recently studied by Fernando and Gamalath [8]. Their applications are of great interest for the protection of high-sensitive devices or the human eyes against intense laser irradiation [9]. The reader will find in [9] a review on optical limiters consisting of inter alia in 1D nonlinear PC, as well as numerous references on the evolution of limiting materials and optical limiting devices.

The disturbances associated with manufacturing errors have been investigated numerically here for our PC-based 2D all-optical limiter design, by randomly varying both the diameters and the positions of the cylinders constituting the structure with defect. Initially, the influence of these disturbances was dissociated to analyze the impact on the structure's behavior. Then, we combined the disturbances of diameters and positions. The obtained results revealed that the transmission for two typical nonlinear levels is not really affected.

## 2. THEORY

We have modeled a 2D PC consisting of  $N=20 \times 5$  parallel cylinders in  $\text{TiO}_2$  material, periodically spaced with a triangular geometry (Fig. 1). Fabricated PCs based on cylinders of several wavelengths in length behave in the same way as infinitely long 2D rods [5]. The presence of a larger ZnO cylinder, inserted in

the middle of the structure, forms a defect, whose mode exhibits a high Q-factor transmission peak. The triangular array is constituted by 100 nm diameter  $\text{TiO}_2$  rods spaced every 240 nm in the Y-direction with a defect made with a 200 nm diameter ZnO rod (Fig. 1).

The theory used here is essentially a Fourier decomposition of the scattered field. The Multi Scattering Method (MSM) theory deals with a set of parallel cylinders illuminated by a plane wave. For each point P in space, the field is decomposed into a sum of the incident field on the  $l$ th cylinder and the scattered field by this cylinder. This incident field is then decomposed into a sum of the scattered fields by all other cylinders in the PC plus the incident wave exciting the PC sample [10].

We use a set of Fourier-Bessel bases centered on each cylinder to rewrite these scattered fields. For the incident wave, we have modeled a laser beam with a waist of  $2 \mu\text{m}$  using some tricks [11]. The transmission is assumed to be equal to the mean of the field, on a pixel line of  $1 \mu\text{m}$  length, placed at one wavelength behind the PC. The results were confronted with other methods, with a perfect agreement for perfect 2D PC and 2D PC with a defect. Fig. 2 shows a comparison between our method and a commercial software from Ansys for the perfect 2D PC.

The bandgap of our structure appears in the visible range from  $0.46 \mu\text{m}$  to  $0.7 \mu\text{m}$  (Fig. 3).

For linear ZnO which corresponds to a low incident laser beam intensity, a high-intensity peak ( $-1 \text{ dB}$ ) appears at  $0.527 \mu\text{m}$  in the center of the band gap (Fig. 3). As expected, this peak revealed in the figure is not affected by the incidence of the beam in the  $X$ - $Y$  plane.

The map of the electric field was calculated for a  $0.527 \mu\text{m}$  laser beam at normal incidence (Fig. 4). The excited defect mode is well highlighted.

For the nonlinear case, we used the method of moments (EFIE — Electric Field Integral Equation) which was applied to evaluate the  $E$  field inside the cylinder, and the permittivity was easily modified [11]. The principle of the EFIE is as follows: the field is decomposed into a scattered field  $E$  plus the incident field. Using the equivalent source theorem, we express the scattered field by current effect  $J$  flowing in each cell

\* Corresponding author: Geraldine Guida (gguida@parisnanterre.fr).

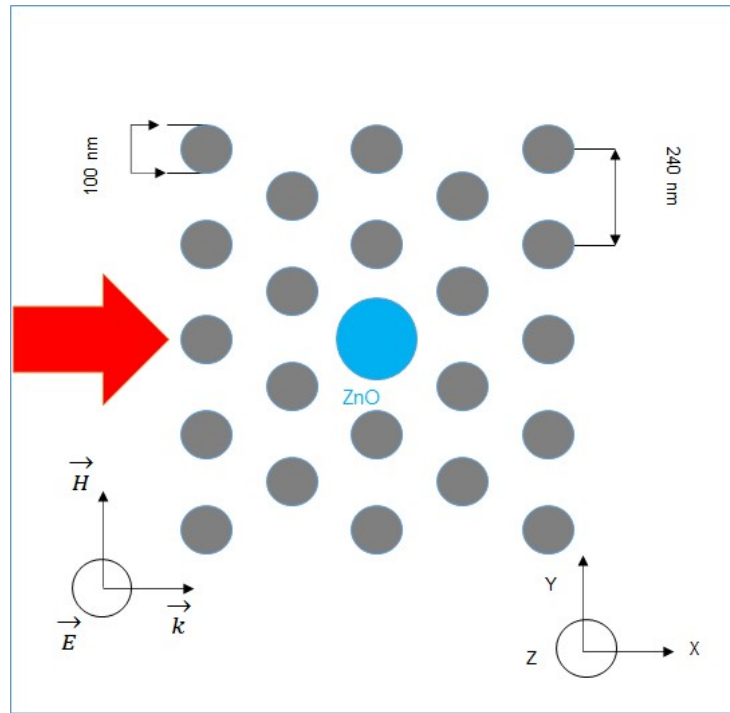


**FIGURE 1.** Design of our triangular lattice of  $\text{TiO}_2$  rods, with the defect of ZnO placed in the middle. The red arrow indicates the direction of the laser light propagation at normal incidence. The 2D PC consists of more than 100 rods (5 in the  $X$  direction) parallel to the  $Z$  axis [10].

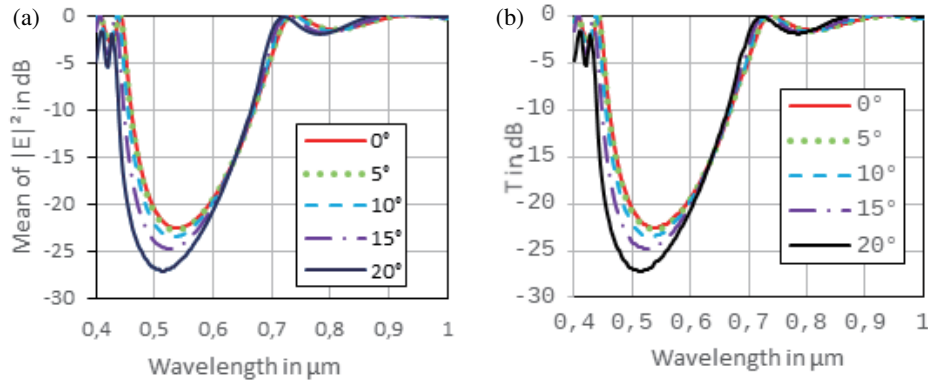


**FIGURE 2.** Calculated transmission of a perfect 2D PC with (a) our method based on Fourier-Bessel bases versus (b) commercial software from Ansys.

of our mesh. The scattered field is then written by convolving the currents using Green's functions (see Equation (1) in [11]) where  $H_0$  is the Hankel's function. To avoid numerical instabilities when the incident wave is in the vacuum, the current  $J$  is replaced by the total field, and the incident field is written as follows:

$$E_{inc}(x, y) = E_z - \omega^2 \epsilon_0 \mu_0 \int \int \frac{1}{4j} \cdot (\epsilon_r(x', y') - 1)) \times E_z(x', y') H_0^{(2)}(kR) dx' dy' \quad (1)$$

with

$$R = \sqrt{(x - x')^2 + (y - y')^2} \quad (2)$$

We discretize field  $E_z$  and permittivities  $\epsilon_r$  in the mesh over small cells (Fig. 5), leading to a matrix system to solve (see Equations (7)–(9) in [11]).

### 3. RESULTS AND DISCUSSION

The interested reader will find a multitude of examples and full details of the whole theory and tricks in [12]. We used cylinders of no more than a few wavelengths, which means that we are working far from the inaccuracy of the EFIE. Several iterations lead to the convergence of the results for a nonlinear material. Indeed, we have taken  $n_{nonlinear} = n_{linear} + \alpha i |E|^2$ , where the values of  $\alpha$  are given in the following section. An iteration process was applied until the convergence [11].

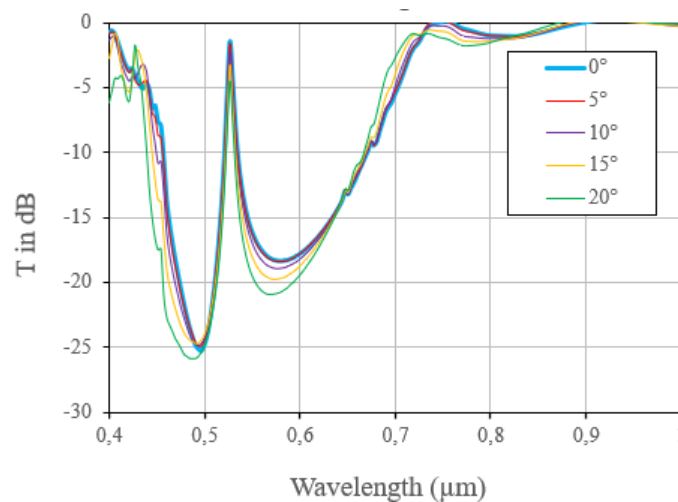


**FIGURE 3.** Transmission in dB versus wavelength in  $\mu\text{m}$ . Defect peak in the visible range (at  $0.527 \mu\text{m}$ ), inside the 2D PC bandgap, for different angles of incidence [10].

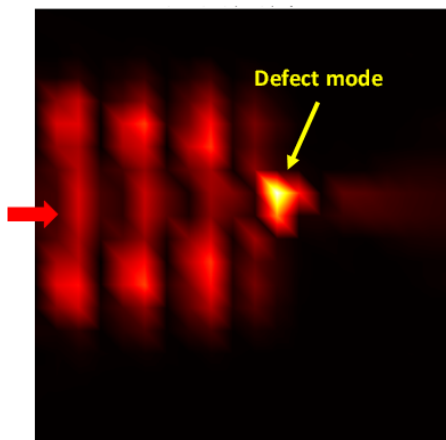


**FIGURE 4.** Map of the electric field  $|E|$ . The laser beam of  $1 \mu\text{m}$  large waist comes from left to right (red arrow).

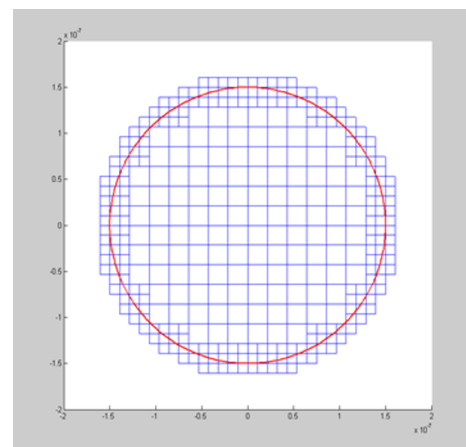


**FIGURE 5.** Mesh of a cylinder by using the method of moments.

Firstly, we calculated the transmission for the defect structure disturbed with different random diameters applied at each rod. The following transmission spectra are focused around the defect mode peak in the visible bandgap from  $0.45 \mu\text{m}$  to  $0.65 \mu\text{m}$  (Fig. 6). We have assumed a hypothesis of ergodicity, for which a mean over a large number of realizations/samples is equivalent to a large one. The number of samples used in this paper is 10, which is a good tradeoff for the time required for numerical simulations. We used random disturbance on diameters of  $\pm 5\%$ ,  $\pm 10\%$ , and  $\pm 15\%$ . The worst case in real manufacturing is estimated at  $\pm 10\%$ . As shown in Fig. 6, the disturbances attenuated the transmission peak from  $-1 \text{ dB}$  to  $-4 \text{ dB}$ , but this new transmission level remains unchanged from weak to strong disturbances. Nevertheless, the shape of the peak is slightly enlarged as the percentage of errors increases.

In a second step, we randomly disturbed only the cylinder positions, for the same percentage of disturbances as previously:  $\pm 5\%$ ,  $\pm 10\%$ , and  $\pm 15\%$ . The random perturbations are on both the  $X$  and  $Y$  axes. The mean over 10 different samples is

plotted in Fig. 7. This figure shows that the effect of this disturbance is more significant than for the diameter disturbance. Indeed, the curves are very jagged. The transmission level of the peak is reduced by  $3 \text{ dB}$ , but the shape of the peak is also really affected. Disturbing the positions deals with a variation in the thickness of the air surrounding the defect, then enlarges or reduces it. As a consequence, several peaks appear at different wavelength values, in the vicinity of the “perfect” peak (peak appearing when no disturbances are taken into account). This result is surprising, as we expected a behavior closer to the one of diameter disturbances shown in Fig. 6.

Finally, to be as close as possible to a PC manufacturing error, we have calculated the transmission for a random  $\pm 10\%$  disturbance on both diameters and positions, which corresponds to the real worst case in the optical domain (Fig. 8). Once again, position perturbations predominate over diameter ones. Moreover, the peak is enlarged compared to the previous cases. In the final section, we calculated the nonlinear effect on this peak as the laser intensity increases. The role of the nonlin-

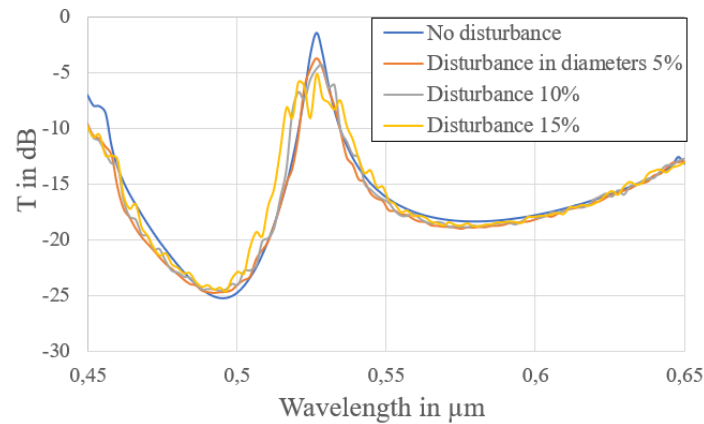


**FIGURE 6.** Transmission (dB) for different diameter disturbance values, means over 10 different realizations.

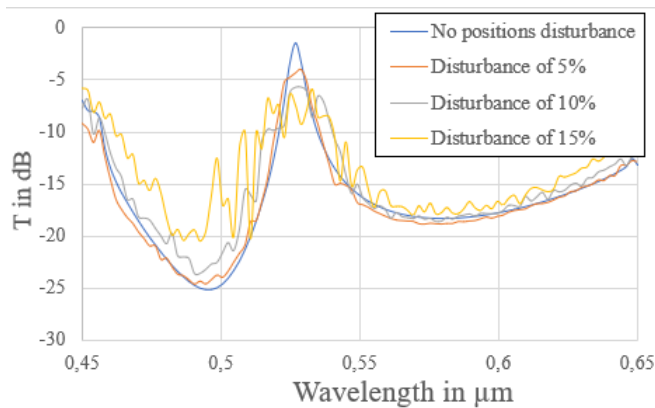


**FIGURE 7.** Transmission for different position disturbances values, means over 10 different realizations.

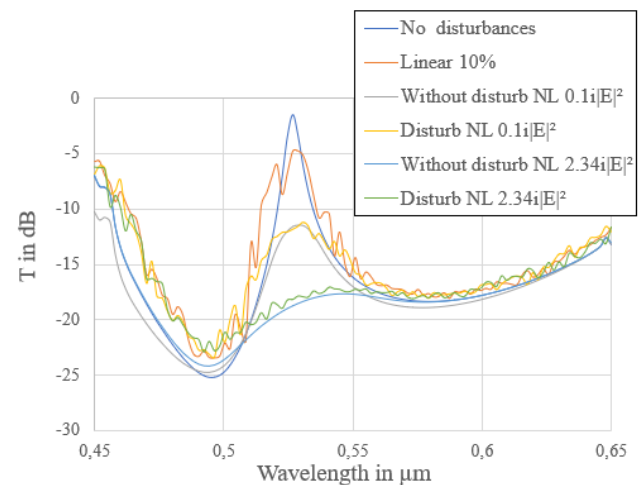


**FIGURE 8.** Transmission spectra for different position and diameter disturbances values, means over 10 different realizations, linear and non-linear cases.

earity of the ZnO cylinder is to drastically reduce the intensity of the peak, in order to obtain an efficient all-optical limiter. We have extracted the ZnO parameters, for an intermediary case of TPA effect and for its extreme case as reported in an experimental study [13]. The imaginary parts of the permittivity vary with incident intensity as  $\alpha \cdot i \cdot |E|^2$  where  $\alpha$  can reach a value of 2.34 for a high-power laser in the wavelength range used in this study. This high level is only 450 MW/cm<sup>2</sup>, which is not very intense considering that attenuation would be more important for higher intensities. The attenuation due to nonlinearity on the peak is greater than -10 dB than the linear case for  $\alpha = 0.1$  and greater than -15 dB for  $\alpha = 2.34$ . Contrarily to the linear case, the disturbed nonlinear case reveals a behavior extremely similar to the undisturbed case, both in terms of peak amplitude and width. This behavior can be explained by the fact that the nonlinearity effect is stronger than disturbance one and highly affects the peak transmission level.

#### 4. CONCLUSION

In summary, a disturbed all-optical model based on a 2D PC with a defect mode has been studied in this paper. This defect was placed in the middle to create a high transmission peak in the visible bandgap. The bandgap extends from 0.46 μm to 0.70 μm, and the peak appears at 0.527 μm. Random errors can occur during structure fabrication. We randomly disturbed both cylinder positions and their diameters for different disturbances percentages:  $\pm 5\%$ ,  $\pm 10\%$ , and  $\pm 15\%$ . We have numerically demonstrated that large  $\pm 10\%$  random position disturbances affect the defect peak that appears at 0.527 μm in the bandgap, more than for  $\pm 10\%$  random diameter disturbances. Nevertheless, the nonlinearity leading to all-optical limiting is not affected by all these disturbances, and this result is particularly interesting for envisaging the fabrication of this type of 2D PC structure for all-optical limiting.

## REFERENCES

- [1] Joannopoulos, J. D., S. G. Johnson, J. N. Winn, and R. D. Meade, *Photonic Crystals: Molding the Flow of Light*, 2nd ed., Princeton University Press, 2008.
- [2] Guida, G., "Numerical studies of disordered photonic crystals," *Progress In Electromagnetics Research*, Vol. 41, 107–131, 2003.
- [3] Fan, W., Z. Hao, Z. Li, Y. Zhao, and Y. Luo, "Influence of fabrication error on the characteristics of a 2-D photonic-crystal cavity," *Journal of Lightwave Technology*, Vol. 28, No. 10, 1455–1458, 2010.
- [4] Kim, H., S. Noda, B.-S. Song, and T. Asano, "Determination of nonlinear optical efficiencies of ultrahigh-Q photonic crystal nanocavities with structural imperfections," *ACS Photonics*, Vol. 8, No. 10, 2839–2845, 2021.
- [5] Guida, G., T. Brillat, A. Ammouche, F. Gadot, A. D. Lustrac, and A. Priou, "Dissociating the effect of different disturbances on the band gap of a two-dimensional photonic crystal," *Journal of Applied Physics*, Vol. 88, No. 8, 4491–4497, 2000.
- [6] Sidibe, A., F. Gadot, B. Belier, G. Bordier, A. Ghribi, A. Tartari, D. Cammilleri, M. Piat, J. Martino, and F. Pajot, "Robustness of the behavior of microstrip lines loaded with disordered complementary split ring resonators," in *2013 Loughborough Antennas & Propagation Conference (LAPC)*, 530–533, Loughborough, UK, Nov. 2013.
- [7] Lin, H. B., R. J. Tonucci, and A. J. Campillo, "Two-dimensional photonic bandgap optical limiter in the visible," *Optics Letters*, Vol. 23, No. 2, 94–96, Jan. 1998.
- [8] Fernando, M. P. and K. W. Gamalath, "Modelling all-optical switching and limiting properties of alas photonic crystals," *International Letters of Chemistry, Physics and Astronomy*, Vol. 77, 1–14, Jan. 2018.
- [9] Gadhwal, R. and A. Devi, "A review on the development of optical limiters from homogeneous to reflective 1-D photonic crystal structures," *Optics & Laser Technology*, Vol. 141, 107144, 2021.
- [10] Bonnefois, J. J., G. Guida, and A. Priou, "A new multiple scattering method application: Simulating an infinite 2D photonic crystal by analyzing, sorting and suppressing the border effects," *Optics Communications*, Vol. 251, No. 1-3, 64–74, 2005.
- [11] Gadot, F., R. Hamié, and G. Guida, "All-optical limiter photonic crystal with two-photon absorption," *Journal of the Optical Society of America A*, Vol. 39, No. 8, 1442–1448, 2022.
- [12] Bonnefois, J., "Modélisation d'effets non linéaires dans les cristaux photoniques, application à la limitation optique," Ph.D. dissertation, Université Paris Nanterre, France, 2006.
- [13] Valligatla, S., A. Chiasera, S. Varas, P. Das, B. N. S. Bhaktha et al., "Optical field enhanced nonlinear absorption and optical limiting properties of 1-D dielectric photonic crystal with ZnO defect," *Optical Materials*, Vol. 50, 229–233, Dec. 2015.